ELSEVIER

Contents lists available at ScienceDirect

Journal of Alloys and Compounds

journal homepage: http://www.elsevier.com/locate/jalcom



Thermoelectric performance of Cu₂Se doped with rapidly synthesized gel-like carbon dots



Cagri Y. Oztan ^a, Bejan Hamawandi ^b, Yiqun Zhou ^c, Sedat Ballikaya ^d, Muhammet S. Toprak ^b, Roger M. Leblanc ^c, Victoria Coverstone ^a, Emrah Celik ^{a, *}

- ^a Department of Mechanical and Aerospace Engineering, University of Miami, USA
- ^b Department of Applied Physics, KTH Royal Institute of Technology, SE 106 91, Stockholm, Sweden
- ^c Department of Chemistry, University of Miami, USA
- ^d Department of Physics, Istanbul University, 34135, Istanbul, Turkey

ARTICLE INFO

Article history:
Received 28 August 2020
Received in revised form
23 October 2020
Accepted 9 November 2020
Available online 12 November 2020

Keywords: Thermoelectric Carbon dots Copper selenide High efficiency

ABSTRACT

As an earth-abundant, inexpensive and non-toxic compound, Copper Selenide (Cu₂Se) is a frequently investigated material for thermoelectric (TE) conversion applications. In this research, stoichiometric Cu₂Se compounds were systematically doped with gel-like Carbon Dots (CDs), that were fabricated using a rapid and straightforward solvothermal method, at weight ratios of 2, 5 and 10%. The resultant ingots were spark plasma sintered and their TE performance was characterized. Scanning electron microscopy (SEM), energy dispersive X-Ray spectroscopy (EDX) and powder X-ray diffraction (PXRD) were used to correlate the microstructure to the TE properties. Based on these measurements, CD doping strategy on Cu₂Se yielded highly compacted, single phase grains with minimal oxidation. Characterization demonstrated a continuous enhancement of TE figure of merit (ZT) to a maximum of 2.1 at the optimum dopant ratio of 2 wt %. This enhancement was mainly due to the energy filtering effect of CD interfaces along the grain boundaries, and phonon scattering which increased the Seebeck coefficient and reduce the thermal conductivity. Doping beyond 2 wt% was recorded to inhibit this improvement. This research paved the path towards broader utilization of rapidly fabricated CDs to enhance TE conversion performance.

© 2020 Elsevier B.V. All rights reserved.

1. Introduction

Due to its reliable, stable, silent and maintenance-free nature, the concept of thermoelectric (TE) power generation stands out as a promising solution to convert waste-heat into electricity. Today, TE devices are successfully used in numerous applications such as wearable electronics [1,2], albeit in a limited scale; since certain constraints such as low conversion efficiency and the need for materials with rare-earth abundance seriously impede their potential for wider scale utilization. The efficiency of a TE material is represented by the dimensionless figure of merit (ZT), which is specified as $ZT=(S^2\sigma T/k)$, where S, σ , T and k denote Seebeck coefficient, electrical conductivity, absolute temperature and thermal conductivity, respectively [3]. It is a requirement that an ideal TE material possesses high power factor ($S^2\sigma$) and low thermal conductivity. Yet, due to the trade-off relations in transport parameters,

* Corresponding author. E-mail address: e.celik@miami.edu (E. Celik). attaining a *ZT* value of >2 is considered as a serious challenge for the TE community to overcome [4]. In addition to high conversion efficiency, high structural stability with minimized fluctuation in conversion efficiency is desired to ensure reliable operability for a thermoelectric material [5].

Since the majority of the previous studies has targeted the improvement of ZT, the search of replacing rare TE materials with the earth-abundant ones has been of ancillary concern [6]. Pursuant to this effort, numerous compounds such as SnSe, SnSi, Mg₂Sn, InSb, PbS, CoSb₃, Zn₃Sb₄, CuS, CuFeS₂ Cu₂Se and Mg₂Si have been investigated [7–26]. Among these, Cu₂Se is a p-type transition metal chalcogenide and has stood out as an attractive material due to its favorable TE performance in mid-temperature ranges and low thermal conductivity [27–31]. TE figure of merit for Cu₂Se compounds are obtained at a range of 1-2-2.0 for the medium temperature ranges (800–1000 K) [32]. This ZT range is comparable to other commonly studied TE materials with high ZT, such as skutterudites [33], GeTe, SnSe and PbQ (Q=Te, Se, S) [34–40]; but earth-abundant and environment-friendly properties of the

constituents of Cu₂Se pave the path towards wider adaptation of this compound. Despite its high thermoelectric performance, low toxicity and high abundance, Cu₂Se has intrinsic properties which may potentially limit its certain applications as a thermoelectric compound. Cu₂Se suffers from fast migration of Cu ions and evaporation of Se under high temperatures which lead to deterioration of its composition [41,42]. In addition, Cu₂Se shows temperature dependent-phase transformation which needs to be taken account in terms of its mechanical, thermal end electrical performance.

Cu₂Se offers highly tailorable thermoelectric performance, which makes it a suitable candidate for material engineering strategies such as band structure engineering and nanostructuring [43,44]. Among these, nanostructuring has been used as a favorable strategy to enhance ZT of Cu₂Se where thermal conductivity is reduced via phonon scattering phenomenon due to the presence of precipitated nanoparticles within the material matrix. In this regard, Yang et al. investigated the effect of spark plasma sintered βphase Cu₂Se nanostructures on TE properties where they reported an increase in blocking of intermediate to short wavelength phonons resulting in a maximum ZT of 1.82 at 850 K [45]. Another attempt involving such a strategy was reported by Zhao et al. where melt-solidified Cu₂Se nanocrystalline solid samples doped with graphite marked tremendously high ZT values of more than 2.4 over 850 K, owing to the high density of interfaces stemming from nanoscale grains [46-48]. On the other hand, the unorthodox strategy of hierarchical nanostructuring in Cu_2Se via α to β phase transition has been reported to evince a promising maximum ZT of 2.0 at 900 K by Tafti et al. [32]. In a successful attempt where SiC nanoparticles were used as dopants by Lei et al. for Cu₂Se where a ZT of 2.0 at 875 K with 0.05 wt% SiC was reported [49]. In another research, multi-walled carbon nanotubes (CNTs) within Cu₂Se were used by Nunna et al. where a high ZT of 2.4 at 1000 K was reportedly achieved, due to the reduction in lattice thermal conductivity [50]. Another remarkably high ZT of 2.14 at 973 K was reported by Hu et al. where lithium doping was used to create nanoporous structure of Cu_{1.98}Li_{0.02}Se and lower thermal conductivity [51]. Hu et al. also investigated the doping of Cu₂Se compounds with carbon dots [52] where they reported that the hot-pressed Cu₂Se doped with CDs enhanced ZT to 1.98 with a CD dopant ratio of 0.8 wt %. Despite the significant enhancement of ZT in this study, limited production yield of CDs using the microwave-assisted fabrication stands as a limitation. Besides, investigating the effects of higher doping concentrations is required for a holistic understanding of CDs on Cu₂Se.

Therefore, the motivation of study is to further increase the TE performance of Cu₂Se using a novel nanomaterial as dopant: gellike carbon dots which were fabricated using a facile, rapid and low-energy synthesis method where 1,2-ethylenediamine (EDA) and citric acid are used as precursors for high doping ratios (2, 5, 10 wt%). Scalability of nanostructured thermoelectric materials is a great challenge limiting the wider usage of these materials especially at these high doping ratios. The solvothermal method used in this research, however, yields higher production volumes of CD nano dopants which can be a remedy to achieve scalable nanostructured thermoelectric materials. Hence, this robust manufacturing technology has potential to significantly enhance the use CD-doped Cu₂Se as efficient TE materials in wide range of energy conversion applications.

2. Materials and methods

2.1. Synthesis of gel-like CDs

To prepare gel-like CDs, deionized water was initially purified by a Modulab 2020 water purification system purchased from

Continental Water System Corporation (San Antonio, TX, USA). The deionized water had a pH of 6.62 ± 0.30 , surface tension of $72.6~\text{mN}~\text{m}^{-1}$ and resistivity of $18~\text{M}\Omega~\text{cm}$ at $25.0\pm0.5~\text{C}$. Subsequently, Argon gas was used to remove O_2 from the solvothermal system. Then, 5~mL of 1,2-ethylenediamine (EDA) was transferred into a 50~mL, round-bottom flask and heated with constant stirring in an oil bath on a hot plate (Chemglass, OptiMag-st). When the temperature reached 160~C, 1~g of citric acid was added with vigorous stirring, and the reaction sustained for 50~min when complete dissolution of citric acid in EDA was ensured. After cooling the system for 15~min to the room temperature, the gel-like CDs were deposited at the bottom of the flask. The remaining EDA was then rinsed out using acetone.

2.2. Synthesis and consolidation of Cu₂Se/CDs

For the synthesis of Cu₂Se, Cu (99.9999% shot from Sigma Aldrich) and Se (99.999% powder from Sigma Aldrich) precursors were stoichiometrically mixed in a glove box. Then mixed were loaded in graphite-coated quartz tubes and sealed under a pressure of 10^{-3} torr. Sealed quartz tubes were placed in a furnace and heated up to 1150 °C at a rate of 1 °C/min, followed by soaking for 12 h to achieve thorough mixing. Subsequently, temperature was reduced to 800 °C at a rate of 4 °C/min where it was maintained for 10 days. Later, the furnace was turned off for a cooldown to room temperature. Resultant ingots were loaded into the glove box where they were ground into fine powders. Fine powders were then mixed with Gel-like CDs according to ratios of 0, 2, 5 and 10% by weight. Each mixture was then blended with ball milling under 200 rpm speed of rotation for 2 h to obtain homogenous mixture. The solution was then loaded into the 12.7 mm graphite die for spark plasma sintering. The powders were cold pressed under 50 MPa which was later reduced to 10 MPa. At this pressure level, samples were heated at a rate of 50 °C/min up to 450 °C, and the uniaxial pressure was readjusted to 50 MPa followed by isothermal/ isobaric hold. Finally, the compacted structure was cut into disks and prismatic bars using a diamond blade to measure thermal diffusivity and transport properties, respectively.

2.3. Structural and thermoelectric analysis

All measurements were performed over the temperature range of 300-873 K. Electrical conductivity and Seebeck coefficient of the samples were measured by using a commercial Ulvac-ZEM 3, M8 device. Thermal conductivity (k) values were calculated in accordance with $k = D.\rho.C_p$ equation, where D, ρ and C_p represent thermal diffusivity, density of mass and specific heat capacity, respectively. Thermal diffusivity was measured using a commercial laser flash thermal diffusivity device LFA 1000 from Linseis, whereas specific heat was measured using a differential scanning calorimeter (Linseis-PT1000). Density of the specimens were obtained with Archimedes' method. Densities were obtained as 6.17 gr/cm³, 5.70 gr/cm³, 5.63 gr/cm³ and 6.08 for Pure Cu₂Se, Cu₂Se + 2 wt% CDs, Cu₂Se + 5 wt% CDs, and Cu₂Se + 10 wt% CDs respectively. Phase purity of samples was characterized via X-ray diffraction pattern by Rigaku Ultima 4 diffractometer. Scanning electron microscopy (SEM) and Energy-dispersive X-ray spectroscopy (EDX) analyses were carried out using a FEI Nova 200 device to analyze the particle morphology and composition of the spark plasma sintered samples and further interpret the TE performance. The surface morphology of the gel-like CDs was characterized via a Transmission Electron Microscopy (TEM) device (JEOL 1200X) TEM where a drop of CDs aqueous dispersion was placed on a carboncoated copper grid and air dried. Spark plasma sintered samples were mechanically loaded until fracture and were positioned on copper tape to prevent overcharging.

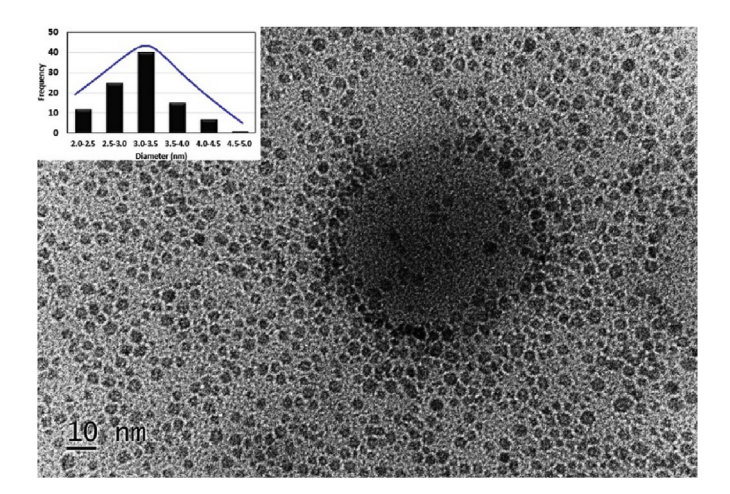


Fig. 1. TEM micrograph of Gel-Like CD-s with the histogram of particle size distribution.

3. Results

3.1. Morphology of the as-synthesized gel-like CDs

The TEM image of the as-synthesized gel-like CDs is provided in Fig. 1 where the inset depicts the size distribution of 100 dots. The TEM micrograph suggests adequate dispersion with minimal aggregation and minor variations in the particle size, pointing out to sufficient carbonization of the gel-like CDs during the synthesis process. The gel-like CDs exhibited quasi-spherical geometry with a narrow Gaussian size distribution of 3.0-3.5 nm. The minimal aggregation of the CD-s was observed to contribute to homogenous dispersion of these nano inclusions within the spark plasma sintered Cu₂Se matrix, upon which isotropic phonon scattering emanated. This was subsequently evidenced by the SEM imaging of the sintered samples.

3.2. Structural analysis

Fig. 2a provides the data for the PXRD analysis. According to the PXRD results, Cu_2Se samples exhibited no impurity where single phase monoclinic Cu_2Se structures (JCPDS PDF no: 00-027-1131) were detected in the material which is in good agreement with the reported literature data [53]. The purity of the samples was further confirmed with the EDX data given in Fig. 2b. In all samples, Cu:Se weight ratio remained approximately the same and only a small trace amounts of oxygen were detected, which might be formed

during the ball milling process of the samples. Although the oxidation in the specimens was found to be minimal, the highest oxygen level was found in the pure Cu_2Se samples and the lowest oxidation was observed in Cu_2Se samples doped with 10% CDs. Lower affinity of the CD-doped specimens to oxidation compared to the pure samples was beneficial to minimize contamination, which is a precursor of potentially high levels of electrical conductivity. Meanwhile, it is noteworthy that the molar ratios Cu:Se of the compounds evinced slight fluctuation, due to the presence of CDs as shown by the Cu/Se molar ratio chart (Fig. 2c) acquired from the EDX analysis. Fig. 3 shows the elemental maps of the 2%, 5% and 10% CD doped specimens. These maps show that copper, selenium and carbon signals overlap. In other words, these elements exist at the same locations without any visible phase separation.

SEM micrographs of the spark plasma sintered samples are provided in Fig. 4. Pure Cu_2Se sample shows highly compacted crystalline structure. However, the crystallinity of samples and the layer formation decrease with the inclusion of CDs. As it can clearly be seen in Fig. 4c and d, increasing concentration of CDs lead to a synergetic increase in the boundary thickness. Despite the lack of a clear evidence to explain this, it may be concluded that the CDs may have infused deep into the matrix, acting as obstacles that prevented Cu mobility which eventually inhibits the formation of larger grains. This can further be corroborated with the decreasing mass density of the CDs doped samples. This likely scenario also concurs with the results reported by Hu et al. [24], where the morphology texture of samples has strong effect on transport properties.

3.3. Thermoelectric characterization

Fig. 5a shows the variation of the Seebeck coefficient as a function of temperature for all samples. The positive sign of Seebeck coefficient confirms that all samples show a p type thermoelectric behavior. Seebeck coefficient increases with the inclusion of CDs. This might be attributed to the low-energy carrier filtering effect emanated by the existence of CDs barriers, which have significant influence on carrier transport characteristics [54,55]. Energy filtering effect and the increase of Seebeck coefficient due to the CD addition has been reported by Hu et al. [52]. In this previous study, it was reported that CD addition would lead to filtering of low-energy carriers by the energy barrier while high-energy carriers are allowed to pass. Although this would reduce the electrical conductivity, the increase in Seebeck coefficient surpasses this reduction leading to overall increase in power factor and the figure of merit as described in the next section. Addition of CDs by more than 2 wt%, however, was recorded to suppress Seebeck coefficient

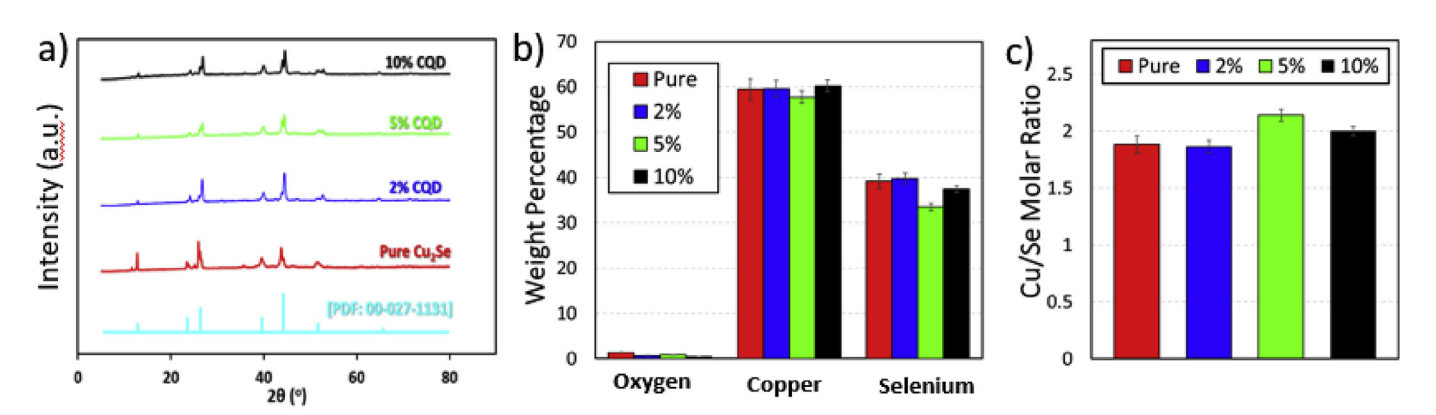


Fig. 2. Phase and elemental analysis of each pure and CD doped Cu₂Se samples: a) PXRD Data, b) Elemental EDX analysis, c) Molar ratio of Cu/Se in EDX analysis.

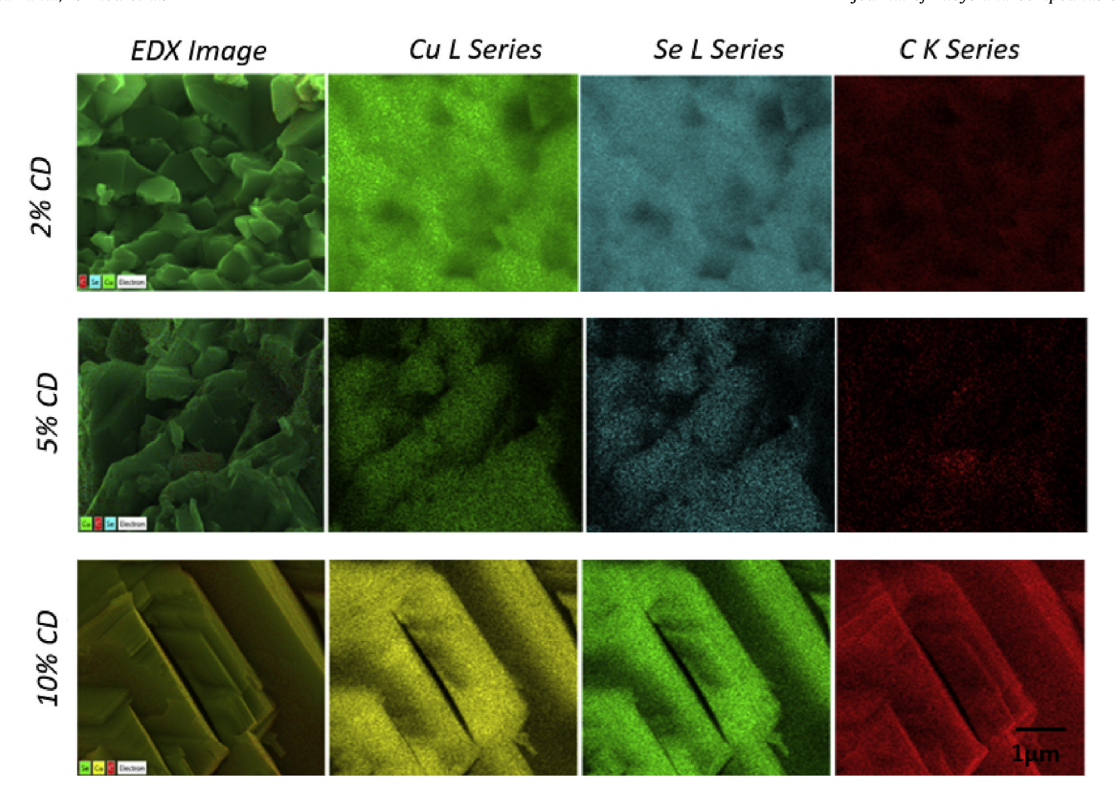
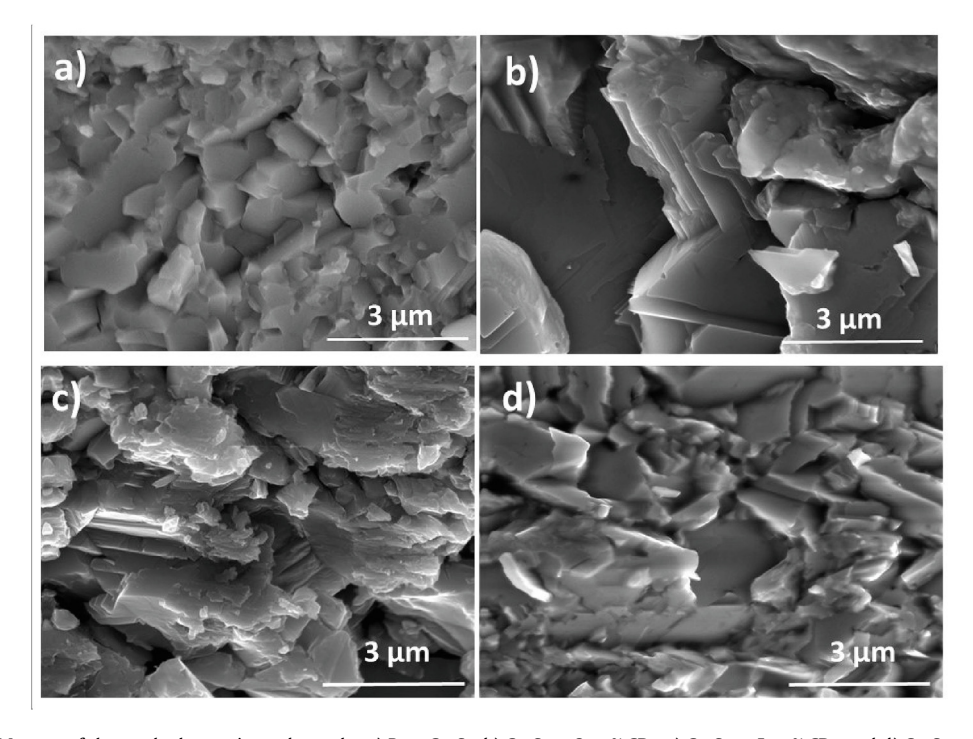


Fig. 3. EDX elemental maps for copper, selenium and carbon for the CD specimens.



 $\textbf{Fig. 4.} \ \ \text{SEM Images of the spark plasma sintered samples a) Pure \ Cu_2Se, \ b) \ Cu_2Se + 2 \ wt\% \ CDs, \ c) \ Cu_2Se + 5 \ wt\% \ CDs, \ and \ d) \ Cu_2Se + 10 \ wt\% \ CDs.$

enhancement due to the loss of coherence in the filtering, marking this ratio as the optimum for the Seebeck coefficient. Highest Seebeck coefficient attained in these samples was $302 \,\mu\text{V/K}$ at the temperature of 873 K, outpacing the value of $260 \,\mu\text{V/K}$ under the same temperature reported previously [52].

Fig. 4b displays the behavior of electrical conductivity with

temperature for all specimens where a continuously decreasing trend is observed, with an opposite trend to that of the Seebeck coefficient, owing to the inherent properties of semiconductors. However, near 400 K, a sharp peak is observed indicating the phase transition at this temperature which is intrinsic to Cu₂Se material [27,28]. Despite the dramatic reduction of electrical conductivity at

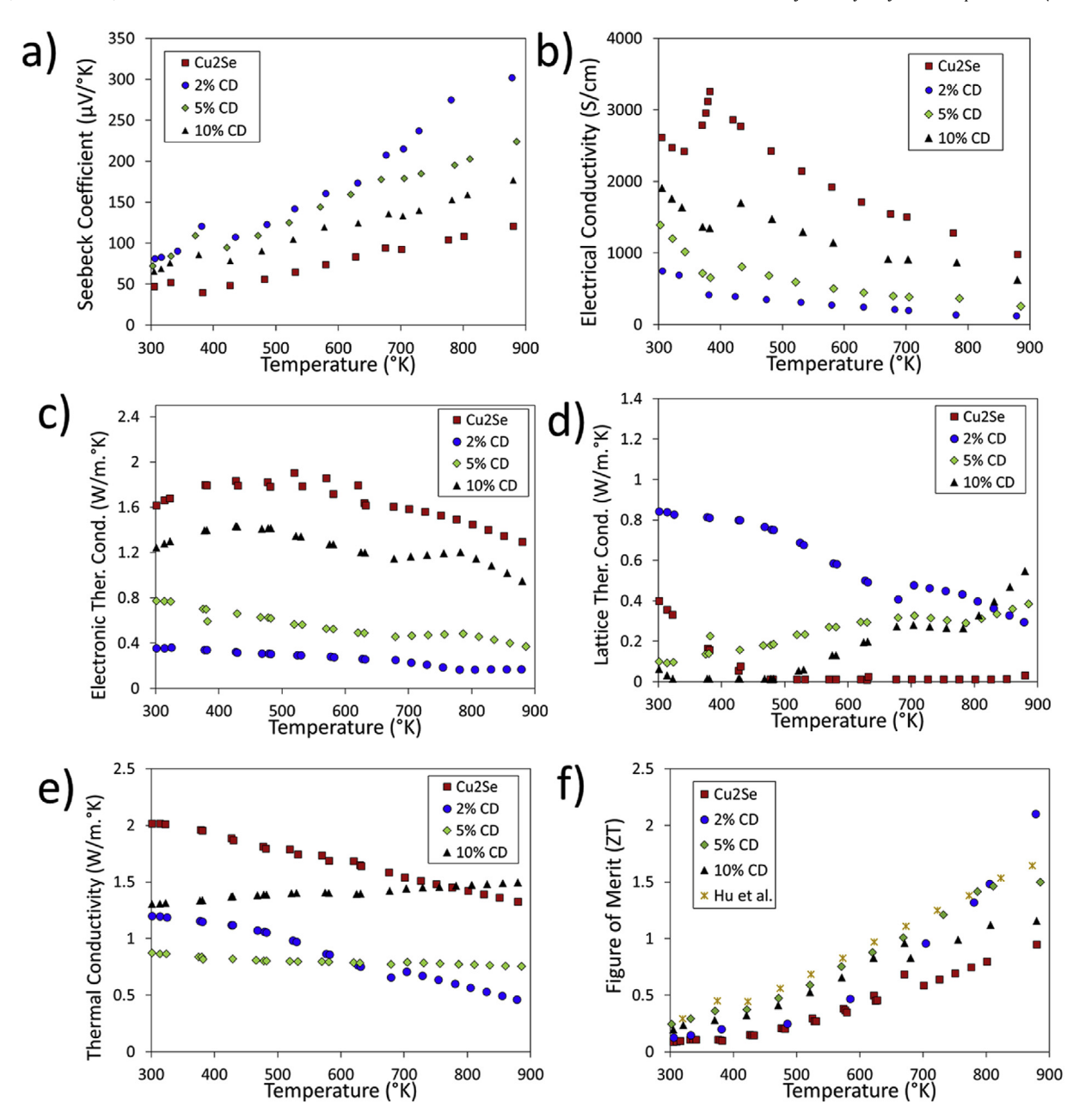


Fig. 5. Variation of TE properties with temperature for pure and CD doped Cu₂Se samples: a) Seebeck Coefficient, b) Electrical Conductivity, c) Thermal Conductivity, d) Dimensionless Figure of Merit, ZT, along with a comparison with the literature data [52].

the dopant ratio of 2 wt%, gradual improvement is recorded as more CDs were intercalated into the Cu_2Se matrix. The highest electrical conductivity in the CD-doped samples (10% doping) was 1976 S/cm at 300 K.

Fig. 4c and d shows the change in each thermal conductivity component, electronic and lattice thermal conductivities ($k = k_e + k_l$), for each sample type. The electronic thermal conductivity was calculated using Wiedemann-Franz Law ($k_e = L\sigma T$), where L is the Lorenz number calculated from equation ($L = 1.5 + \exp[-|S|/116)$). Apart from the samples doped with CD by 2 wt%, lattice thermal conductivity values were observed to be significantly lower than the electronic thermal conductivity. Nonetheless, it is obvious that the presence of CDs capitalizes on reduction of lattice thermal conductivity by acting as low-energy phonon blocking barriers, which is in agreement with the literature [47,56]. Fig. 4e signifies

the change of total thermal conductivity with temperature where the mid/long wavelength phonon scattering due to the addition of CD-nanoparticles is clearly demonstrated, especially at elevated temperatures. This reduction can be ascribed to the energy filtering effect of the CD interfaces along the grain boundaries, which are known to scatter phonons and block low-energy electrons, thereby reducing the thermal conductivity [57,58]. Per this figure it can also be deduced that, increased amount of CD-doping alters the thermal conductivity trend from decreasing to increasing over temperature, and low dopant ratios yield with a declining trend is in good agreement with Hu's work [52]. The variation of calculated dimensionless figure of merit with temperature is shown in Fig. 4f. All CD doped specimens showed superior figure of merit compared to the pure Cu₂Se samples. Specimens doped with 2 wt% CD marked the highest *ZT* values at elevated temperatures (>800 K)

which was mainly due to the increase of the Seebeck coefficient and reduction of thermal conductivity in these specimens. Maximum *ZT* of 2.1 is achieved in this specimen at 880 K which was 2.6 folds higher than that of the undoped Cu₂Se sample. As described in the previous section, lower oxygen affinity of the CD-doped materials can play a part in this efficiency enhancement as well. In terms of comparison to the previous studies, the highest *ZT* of 2.1 attained at 880 K in this study was higher than the majority of the previously reported Cu₂Se [45,49,51] and Cu₂Se-CD hybrid systems [52] remarking the second highest TE figure of merit of Cu₂Se based TE materials at this temperature after the *ZT* reported by Zhao et al. [48].

4. Conclusions

Cu₂Se is a promising TE system due to its earth-abundant constituents and high TE figure of merit for mid-temperature range applications. This study aimed to further enhance the TE conversion efficiency of these materials by doping with CD nanomaterials. Gellike CD nanomaterials were fabricated using a facile and rapid solvothermal method. Cu₂Se powders were doped with these CDs and spark plasma sintered to over fabricate hybrid TE systems. The hybrid systems showed superior TE figure of merit compared to undoped Cu₂Se marking the maximum figure of merit of 2.1 at 880 K with a CD dopant ratio of 2 wt%. To the best of our knowledge, this is the highest figure of merit at this temperature achieved for CD-doped Cu₂Se material systems in literature. The structural analysis conducted on the samples suggested high levels of purity. which is a significant factor that contributed towards the high ZT achieved. Other factors that accounted for this achievement are the synergetic presence of quasi-spherical CD nanoparticles, smaller grain sizes and high density of sintered Cu₂Se matrix which amplified phonon scattering and electrical conductivity. It was concluded that the presence of CD nanoparticles promotes energy filtering effect, which ensured high Seebeck coefficients and reduced thermal conductivity. Therefore, this study establishes the novel methodologies for fabricating gel-like CD-doped Cu₂Se material systems where the scaled-up nano dopant preparation procedures and enhanced TE conversion efficiencies are reported. It is expected that, the outcomes of this study will help wider adoption of Cu₂Se for energy harvesting applications in near future.

CRediT author statement

Cagri Y. Oztan: Conceptualization, manuscript writing.

Bejan Hamawandi: Performing SEM analysis and thermal conductivity calculations.

Yiqun Zhou: CD synthesis and characterization.

Sedat Ballikaya: Fabrication of pure and CD doped Cu2Se specimens and characterization.

Muhammet S. Toprak: Supervising the SEM and thermal conductivity analysis.

Roger Leblanc: Supervising CD synthesis and characterization. **Victoria Coverstone**: Manuscript writing.

Emrah Celik: Overall Research Supervision, Manuscript Reviewing and Editing.

Declaration of competing interest

The authors declare that they have no known competing financial interests or personal relationships that could have appeared to influence the work reported in this paper.

Acknowledgements

This work is supported by the Scientific and Technological Research Council of Turkey (TUBITAK) under the Project Number 216M254 and Scientific Research Projects Coordination Unit of Istanbul University with project number of 35577 and 32641, as well as by the Swedish Energy Agency (Energimyndigheten, 43521–1). Professor Roger M. Leblanc thanks the support from National Science Foundation under the awards of 1809060 as well as CBET-2041413 EAGER.

References

- [1] Y. Wang, M. Hong, W.-D. Liu, X.-L. Shi, S.-D. Xu, Q. Sun, H. Gao, S. Lu, J. Zou, Z.-G. Chen, BiO. 5Sb1. 5Te3/PEDOT: PSS-based flexible thermoelectric film and device, Chem. Eng. J. (2020) 125360.
- [2] M. Dargusch, W.D. Liu, Z.G. Chen, Thermoelectric generators: alternative power supply for wearable electrocardiographic systems, Adv. Sci. 7 (2020) 2001362
- [3] H.J. Goldsmid, Introduction to Thermoelectricity, Springer, 2010.
- [4] K.B. Masood, P. Kumar, R. Singh, J. Singh, Odyssey of thermoelectric materials: foundation of the complex structure, J. Phys. Commun. 2 (2018), 062001.
- [5] P. Jood, R. Chetty, M. Ohta, Structural stability enables high thermoelectric performance in room temperature Ag 2 Se, J. Mater. Chem. 8 (2020) 13024–13037.
- [6] A. Suwardi, L. Hu, X. Wang, X.Y. Tan, D.V.M. Repaka, L.-M. Wong, X. Ni, W.H. Liew, S.H. Lim, Q. Yan, Origin of high thermoelectric performance in earth-abundant phosphide-tetrahedrite, ACS Appl. Mater. Interfaces 12 (2020) 9150–9157.
- [7] N.K. Singh, S. Bathula, B. Gahtori, K. Tyagi, D. Haranath, A. Dhar, The effect of doping on thermoelectric performance of p-type SnSe: promising thermoelectric material, J. Alloys Compd. 668 (2016) 152–158.
- [8] R.D. Schmidt, E.D. Case, L.-D. Zhao, M.G. Kanatzidis, Mechanical properties of low-cost, earth-abundant chalcogenide thermoelectric materials, PbSe and PbS, with additions of 0–4% CdS or ZnS, J. Mater. Sci. 50 (2015) 1770–1782.
- [9] Y.S. Lim, K.-H. Park, J.Y. Tak, S. Lee, W.-S. Seo, C.-H. Park, T.H. Kim, P. Park, L.-H. Kim, J. Yang, Colligative thermoelectric transport properties in n-type filled CoSb3 determined by guest electrons in a host lattice, J. Appl. Phys. 119 (2016) 115104.
- [10] A.S. Mikhaylushkin, J. Nylén, U. Häussermann, Structure and bonding of Zinc Antimonides: complex frameworks and narrow band gaps, Chem. Eur J. 11 (2005) 4912–4920.
- [11] J. Li, Q. Tan, J.-F. Li, Synthesis and property evaluation of CuFeS2— x as earthabundant and environmentally-friendly thermoelectric materials, J. Alloys Compd. 551 (2013) 143—149.
- [12] K. Yuan, J. Wu, M. Liu, L. Zhang, F. Xu, L. Chen, F. Huang, Fabrication and microstructure of p-type transparent conducting CuS thin film and its application in dye-sensitized solar cell, Appl. Phys. Lett. 93 (2008) 132106.
- [13] S. Ballikaya, H. Chi, J.R. Salvador, C. Üher, Thermoelectric properties of Agdoped Cu 2 Se and Cu 2 Te, J. Mater. Chem. 1 (2013) 12478–12484.
 [14] C. Nakhowong, T. Sumpao, T. Seetawan, Synthesis and Characterization of
- [14] C. Nakhowong, T. Sumpao, T. Seetawan, Synthesis and Characterization of Mg2Si Thermoelectric Material, Advanced Materials Research, Trans Tech Publ, 2013, pp. 213–217.
- [15] L. Bertini, C. Stiewe, M. Toprak, S. Williams, D. Platzek, A. Mrotzek, Y. Zhang, C. Gatti, E. Müller, M. Muhammed, Nanostructured Co 1 x Ni x Sb 3 skutterudites: synthesis, thermoelectric properties, and theoretical modeling, J. Appl. Phys. 93 (2003) 438–447.
- [16] J.P. Heremans, The ugly duckling, Nature 508 (2014) 327–328.
- [17] H. Li, X. Tang, Q. Zhang, C. Uher, High performance in x Ce y Co 4 Sb 12 thermoelectric materials with in situ forming nanostructured InSb phase, Appl. Phys. Lett. 94 (2009) 102114.
- [18] A.U. Khan, K. Kobayashi, D.-M. Tang, Y. Yamauchi, K. Hasegawa, M. Mitome, Y. Xue, B. Jiang, K. Tsuchiya, D. Golberg, Nano-micro-porous skutterudites with 100% enhancement in ZT for high performance thermoelectricity, Nano Energy 31 (2017) 152–159.
- [19] N. Tsujii, T. Mori, High thermoelectric power factor in a carrier-doped magnetic semiconductor CuFeS2, APEX 6 (2013), 043001.
- [20] R. Ang, A.U. Khan, N. Tsujii, K. Takai, R. Nakamura, T. Mori, Thermoelectricity generation and electron—magnon scattering in a natural chalcopyrite mineral from a deep-sea hydrothermal vent, Angew. Chem. 127 (2015) 13101—13105.
- [21] V. Zaitsev, M. Fedorov, E. Gurieva, I. Eremin, P. Konstantinov, A.Y. Samunin, M. Vedernikov, Highly effective Mg 2 Si 1 – x Sn x thermoelectrics, Phys. Rev. B 74 (2006), 045207.
- [22] H. Ning, G.D. Mastrorillo, S. Grasso, B. Du, T. Mori, C. Hu, Y. Xu, K. Simpson, G. Maizza, M.J. Reece, Enhanced thermoelectric performance of porous magnesium tin silicide prepared using pressure-less spark plasma sintering, J. Mater. Chem. 3 (2015) 17426–17432.
- [23] H. Anno, M. Hokazono, R. Shirataki, Y. Nagami, Crystallographic, thermoelectric, and mechanical properties of polycrystalline type-I Ba 8 Al 16 Si 30based clathrates, J. Mater. Sci. 48 (2013) 2846–2854.
- [24] B. Hinterleitner, I. Knapp, M. Poneder, Y. Shi, H. Müller, G. Eguchi,

- C. Eisenmenger-Sittner, M. Stöger-Pollach, Y. Kakefuda, N. Kawamoto, Thermoelectric performance of a metastable thin-film Heusler alloy, Nature 576 (2019) 85–90.
- [25] N. Tsujii, A. Nishide, J. Hayakawa, T. Mori, Observation of enhanced thermopower due to spin fluctuation in weak itinerant ferromagnet, Sci. Adv. 5 (2019), eaat5935.
- [26] G. Rogl, P. Sauerschnig, Z. Rykavets, V. Romaka, P. Heinrich, B. Hinterleitner, A. Grytsiv, E. Bauer, P. Rogl, (V, Nb)-doped half Heusler alloys based on (Ti, Zr, Hf) NiSn with high ZT. Acta Mater. 131 (2017) 336—348.
- [27] B. Hamawandi, S. Ballikaya, M. Råsander, J. Halim, L. Vinciguerra, J. Rosen, M. Johnsson, M. Toprak, Composition tuning of nanostructured binary copper selenides through rapid chemical synthesis and their thermoelectric property evaluation, Nanomaterials 10 (2020) 854.
- [28] C. Coughlan, M. Ibanez, O. Dobrozhan, A. Singh, A. Cabot, K.M. Ryan, Compound copper chalcogenide nanocrystals, Chem. Rev. 117 (2017) 5865—6109.
- [29] N. Nandihalli, C.-J. Liu, T. Mori, Polymer based thermoelectric nanocomposite materials and devices: fabrication and characteristics, Nano Energy (2020) 105186.
- [30] Z. Ogorelec, B. Celustka, Thermoelectric power and phase transitions of the non-stoichiometric cuprous selenide, J. Phys. Chem. Solid. 27 (1966) 615–617.
- [31] T.W. Day, K.A. Borup, T. Zhang, F. Drymiotis, D.R. Brown, X. Shi, L. Chen, B.B. Iversen, G.J. Snyder, High-temperature thermoelectric properties of Cu 1.97 Ag 0.03 Se 1+ y, Mater. Renew. Sustain. Energy 3 (2014) 26.
- [32] M.Y. Tafti, S. Ballikaya, A.M. Khachatourian, M. Noroozi, M. Saleemi, L. Han, N.V. Nong, T. Bailey, C. Uher, M.S. Toprak, Promising bulk nanostructured Cu 2 Se thermoelectrics via high throughput and rapid chemical synthesis, RSC Adv. 6 (2016) 111457–111464.
- [33] G. Rogl, A. Grytsiv, K. Yubuta, S. Puchegger, E. Bauer, C. Raju, R. Mallik, P. Rogl, In-doped multifilled n-type skutterudites with ZT= 1.8, Acta Mater. 95 (2015) 201–211.
- [34] H. Wu, L.-D. Zhao, F. Zheng, D. Wu, Y. Pei, X. Tong, M.G. Kanatzidis, J. He, Broad temperature plateau for thermoelectric figure of merit ZT> 2 in phase-separated PbTe 0.7 S 0.3, Nat. Commun. 5 (2014) 1–9.
- separated PbTe 0.7 S 0.3, Nat. Commun. 5 (2014) 1–9.

 [35] R.J. Korkosz, T.C. Chasapis, S.-h. Lo, J.W. Doak, Y.J. Kim, C.-l. Wu, E. Hatzikraniotis, T.P. Hogan, D.N. Seidman, C. Wolverton, High ZT in p-Type (PbTe) 1–2 x (PbSe) x (PbS) x Thermoelectric Materials, J. Am. Chem. Soc. 136 (2014) 3225–3237.
- [36] H. Wang, J. Wang, X. Cao, G.J. Snyder, Thermoelectric alloys between PbSe and PbS with effective thermal conductivity reduction and high figure of merit, J. Mater. Chem. 2 (2014) 3169–3174.
- [37] W.D. Liu, D.Z. Wang, Q. Liu, W. Zhou, Z. Shao, Z.G. Chen, High-performance GeTe-based thermoelectrics: from materials to devices, Adv. Energy Mater. 10 (2020) 2000367.
- [38] M. Hong, W. Lyu, Y. Wang, J. Zou, Z.-G. Chen, Establishing the golden range of Seebeck coefficient for maximizing thermoelectric performance, J. Am. Chem. Soc. 142 (2020) 2672–2681.
- [39] M. Li, M. Hong, X. Tang, Q. Sun, W.Y. Lyu, S.D. Xu, L.Z. Kou, M. Dargusch, J. Zou, Z.G. Chen, Crystal symmetry induced structure and bonding manipulation boosting thermoelectric performance of GeTe, Nano Energy 73 (2020).
- [40] X.L. Shi, X.Y. Tao, J. Zou, Z.G. Chen, High-performance thermoelectric SnSe: aqueous synthesis, innovations, and challenges, Adv. Sci. 7 (2020).
- [41] J.-Y. Tak, W.H. Nam, C. Lee, S. Kim, Y.S. Lim, K. Ko, S. Lee, W.-S. Seo, H.K. Cho, J.-H. Shim, Ultralow lattice thermal conductivity and significantly enhanced near-room-temperature thermoelectric figure of merit in α-Cu2Se through suppressed Cu vacancy formation by overstoichiometric Cu addition, Chem.

- Mater. 30 (2018) 3276-3284.
- [42] S. Ballikaya, Y. Oner, T. Temel, B. Ozkal, T.P. Bailey, M.S. Toprak, C. Uher, Thermoelectric and thermal stability improvements in Nano-Cu2Se included Ag2Se, J. Solid State Chem. 273 (2019) 122–127.
- [43] W.-D. Liu, L. Yang, Z.-G. Chen, Cu2Se thermoelectrics: property, methodology, and device, Nano Today 35 (2020) 100938.
- [44] W.D. Liu, L. Yang, Z.G. Chen, J. Zou, Promising and eco-friendly Cu2X-based thermoelectric materials: progress and applications, Adv. Mater. 32 (2020) 1905703
- [45] L. Yang, Z.-G. Chen, G. Han, M. Hong, Y. Zou, J. Zou, High-performance thermoelectric Cu2Se nanoplates through nanostructure engineering, Nano Energy 16 (2015) 367–374.
- [46] L. Zhao, X. Sun, Z. Lei, J. Zhao, J. Wu, Q. Li, A. Zhang, Thermoelectric behavior of aerogels based on graphene and multi-walled carbon nanotube nanocomposites, Compos. B Eng. 83 (2015) 317–322.
- [47] M. Li, D.L. Cortie, J. Liu, D. Yu, S.M.K.N. Islam, L. Zhao, D.R. Mitchell, R.A. Mole, M.B. Cortie, S. Dou, Ultra-high thermoelectric performance in graphene incorporated Cu2Se: role of mismatching phonon modes, Nano Energy 53 (2018) 993–1002.
- [48] L. Zhao, S.M.K.N. Islam, J. Wang, D.L. Cortie, X. Wang, Z. Cheng, J. Wang, N. Ye, S. Dou, X. Shi, Significant enhancement of figure-of-merit in carbon-reinforced Cu2Se nanocrystalline solids, Nano Energy 41 (2017) 164–171.
- [49] J. Lei, Z. Ma, D. Zhang, Y. Chen, C. Wang, X. Yang, Z. Cheng, Y. Wang, High thermoelectric performance in Cu 2 Se superionic conductor with enhanced liquid-like behaviour by dispersing SiC, J. Mater. Chem. 7 (2019) 7006–7014.
 [50] R. Nunna, P. Qiu, M. Yin, H. Chen, R. Hanus, Q. Song, T. Zhang, M.-Y. Chou,
- [50] R. Nunna, P. Qiu, M. Yin, H. Chen, R. Hanus, Q. Song, T. Zhang, M.-Y. Chou, M.T. Agne, J. He, Ultrahigh thermoelectric performance in Cu 2 Se-based hybrid materials with highly dispersed molecular CNTs, Energy Environ. Sci. 10 (2017) 1928—1935.
- [51] Q. Hu, Z. Zhu, Y. Zhang, X.-J. Li, H. Song, Y. Zhang, Remarkably high thermoelectric performance of Cu 2– x Li x Se bulks with nanopores, J. Mater. Chem. 6 (2018) 23417–23424.
- [52] Q. Hu, Y. Zhang, Y. Zhang, X.-J. Li, H. Song, High thermoelectric performance in Cu2Se/CDs hybrid materials, J. Alloys Compd. 813 (2020) 152204.
- [53] R.D. Heyding, R.M. Murray, The crystal structures of Cu1• 8Se, Cu3Se2, α -and γ CuSe, CuSe2, and CuSe2II, Can. J. Chem. 54 (1976) 841–848.
- [54] A. Pakdel, Q. Guo, V. Nicolosi, T. Mori, Enhanced thermoelectric performance of Bi-Sb-Te/Sb 2 O 3 nanocomposites by energy filtering effect, J. Mater. Chem. 6 (2018) 21341–21349.
- [55] A. Shakouri, C. LaBounty, P. Abraham, J. Piprek, J.E. Bowers, Enhanced thermionic emission cooling in high barrier superlattice heterostructures, in: Thermoelectric Materials 1998 - the Next Generation Materials for Small-Scale Refrigeration and Power Generation Applications, vol. 545, 1999, pp. 449–458.
- [56] Y. Lin, M. Wood, K. Imasato, J.J. Kuo, D. Lam, A.N. Mortazavi, T.J. Slade, S.A. Hodge, K. Xi, M.G. Kanatzidis, Expression of interfacial Seebeck coefficient through grain boundary engineering with multi-layer graphene nanoplatelets, Energy Environ. Sci. (2020).
- [57] A. Soni, Y. Shen, M. Yin, Y. Zhao, L. Yu, X. Hu, Z. Dong, K.A. Khor, M.S. Dresselhaus, Q. Xiong, Interface driven energy filtering of thermoelectric power in spark plasma sintered Bi2Te2. 7Se0. 3 nanoplatelet composites, Nano Lett. 12 (2012) 4305–4310.
- [58] J.P. Heremans, C.M. Thrush, D.T. Morelli, Thermopower enhancement in lead telluride nanostructures, Phys. Rev. B 70 (2004) 115334.